Usage Report for Fiscal Year 2023

Project Title:

Improved hydrodynamical simulations of gamma-ray burst central engines

Name:

○Yuki Takei (1,2), Oliver Just (1,3), and Hirotaka Ito (1)

Laboratory at RIKEN:

(1) Cluster for Pioneering Research, Astrophysical Big Bang Laboratory

(2) Research Center for the Early Universe, School of Science, The University of Tokyo

(3) GSI Center for Heavy Ion Research, Darmstadt, Germany

1. Background and purpose of the project, relationship of the project with other projects

One of the most luminous events in the Universe, short gamma-ray burst (sGRB), has first been confirmed to be associated with the coalescence of binary neutron stars on 17th August 2017 by observation of a gravitational wave (GW) by Laser Interferometer Gravitational-wave Observatory (LIGO) and Virgo, followed by a short gamma-ray burst GRB 170817A at the same location about two seconds later. Furthermore, a kilonova was also observed for the first time, which confirmed that the rapid neutron-capture process (so-called r-process) nucleosynthesis really happens in kilonovae. The successful detection of these signals at the same time (GW, gamma-ray, optical, infrared, etc.) including neutrino emission leads us to a new world of multi-messenger astronomy.

One of the interesting aspects of GRB 170817A is that the opening angle of the relativistic jet is rather narrow (~4°, Mooley et al. 2018, ~3.4°±1°, Ghirlanda et al. 2019), while jets associated with "ordinary" sGRBs exhibit wider opening angles (~16°±10°, Fong et al. 2015). Although there are plenty of theoretical works surveying the parameter dependence on the opening angle (e.g., Bromberg et al. 2011; Mizuta & Ioka 2013; Nagakura et al. 2014; Hamidani et al. 2020), the opening angle of the jet tends to be narrow compared to observations. To our knowledge, what makes this discrepancy remains an open question.

Following the previous project Q22542, we focus on investigating the dependence of the jet opening angle on some parameters, such as the torus mass, ejecta mass, initial opening angle of the jet, and injected energy by conducting a significant amount of hydrodynamical simulations in this project Q23542.

2. Specific usage status of the system and calculation method

We used the same method as the one that was used in the previous related project (see also the report for Q21542). We rewrite the method in the following; For the hydrodynamical simulations, we employ the code AENUS-ALCAR, which solves the special relativistic hydrodynamics equations together with the M1 approximation of neutrino transport on a fixed, Eulerian mesh using Riemann-solver based finite-volume methods.

As we already have results in the previous project, we have consumed only ~5% of the total allocated CPU time to modify some of our hydrodynamical calculations.

3. Result

We investigate the dependence of the jet opening angle $\theta_{\rm core}$ on the injected jet energy L_j, the ejecta mass $M_{\rm ej}$, the torus mass $M_{\rm tor}$, and the initial opening angle θ_j.

We show the temporal evolution of the Lorentz factor Γ for 4 broad types of all calculations in Figure 1. As can be seen from the figure, whether the jet is successfully launched depends on the selected parameters.

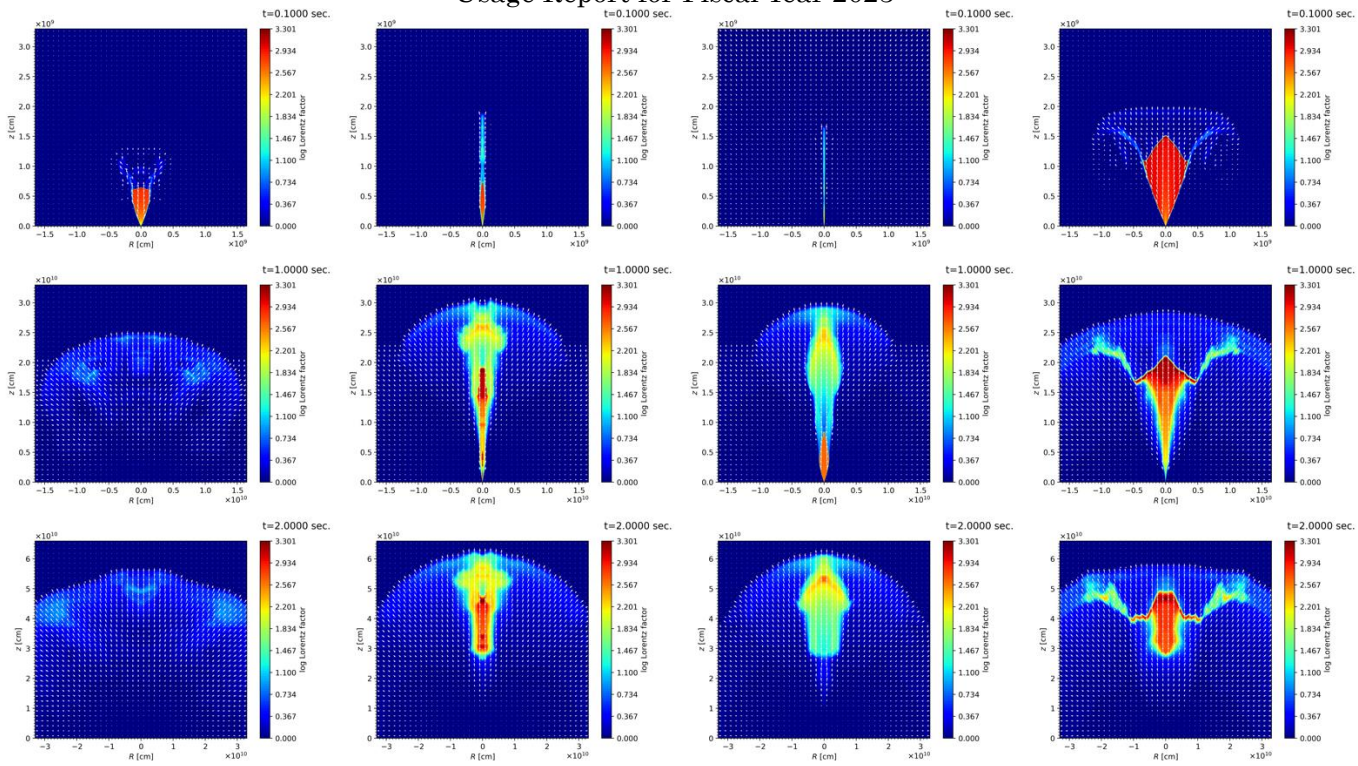

Figure 1: Snapshots illustrating the evolution of the Lorentz factor. We have categorized all calculations into four broad types. The vertical direction represents the time evolution from $t = 0.1$ sec to 2 sec. for the same model. The white arrows indicate the velocity field. The first column from the left shows the model in which the jet fails to launch, while the second, third, and the last columns represent successful jet models.

The first column from the left in this figure represents a jet model not being successfully launched. While Γ exceeds ~100 which characterizes the relativistic jet (Lithwick & Sari 2001) at $t = 0.1$ s, Γ immediately drops to ~10. This event may not be observed as an ordinary SGRB.

The jet models with a torus are categorized in the second column from the left. The most prominent feature appears in the area at the bottom of the jet seen at $t = 1$ s. This feature is caused by the disk wind emerging at $t \sim 0.4$ s ($z < 10^{10}$ cm). Since the jet energy is concentrated at the axis, we can see the energetic core where $\Gamma > 1000$.

If the torus does not exist, the situation drastically changes. From the third column which shows the evolution without the torus, the jet does not become narrower compared to the jet models with the torus.

Finally, the last column represents the uncollimated jet shape with a small ejecta mass and/or higher injecting energy. In this case, the jet is uncollimated if the ambient density is sufficiently small compared to the energy density of the jet. The threshold above which the jet should be collimated is characterized by the following dimensionless parameter (Bromberg et al. 2011),

$$\tilde{L} \equiv \frac{\rho_{\rm jet} h_{\rm jet} \Gamma_{\rm jet}^2}{\rho_{\rm a}},$$

where the subindices jet, a designate the physical quantities related to the jet and ambient medium, respectively, and ρ, h denote the density and specific enthalpy. When $\tilde{L} \gg \theta_j^{-4/3}$, the jet is categorized into this type. In this case, this criterion is satisfied by quite a small density of ambient matter $\rho_{\rm a}$.

Next, we define the jet opening angle to discuss the dependence, although some definitions are used (e.g., Nagakura et al. 2014,; Lamb et al. 2021; Gottlieb et al. 2021). In this work, $\theta_{\rm core}$ is defined by the isotropic equivalent energy $E_{\rm iso}$. Lamb et al. (2021) defines $\theta_{\rm core}$ by $E_{\rm iso}(\theta_{\rm core}) = E_{\rm iso}(\theta = 0)e^{-1}$, while Gottlieb et al. (2021) finds $\theta_{\rm core}$ at the point where $E_{\rm iso}(\theta_{\rm core}) = 0.75E_{\rm iso}(\theta = 0)$. In this work, a similar method is used to define $\theta_{\rm core}$,

$$E_{\rm iso}(\theta_{\rm core}) = E_{\rm iso,max}/x, 2 \leq x \leq 5,$$

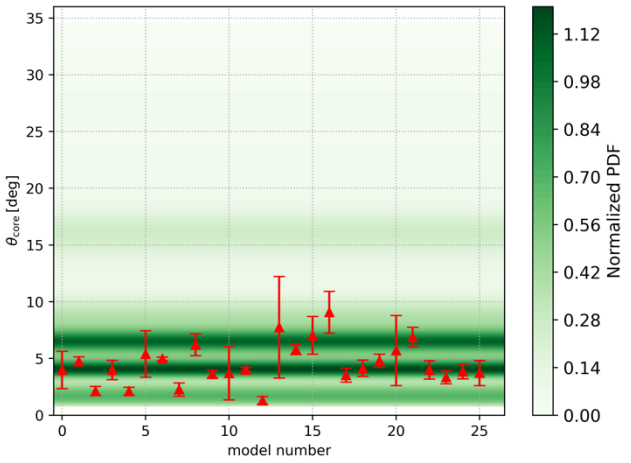

Figure 2: Opening angles of the jet for all models we simulate in this work except for the one model where the jet cannot successfully launch. The horizontal axis denotes the model number. The green contour represents the normalized probability distribution of the opening angle inferred from the afterglow of the jet by Rouco Escrorial et al. (2022). We extract the value of the normalized probability distribution from the left panel of Figure 4.

where $E_{\rm iso,max}$ denotes the maximum value of $E_{\rm iso}$. Since the peak of $E_{\rm iso}$ shifts to > 0 deg, we use $E_{\rm iso,max}$ instead of $E_{\rm iso}(\theta = 0)$. Then $\theta_{\rm core}$ is a function of x, plotted with error bars in Figure 2. We can reproduce the typical opening angles of $\theta_{\rm core} \leq 10$ deg, while the broader angles cannot be explained by the parameter spaces we explore.

4. Conclusion

We investigate the dependence of the jet opening angle on various parameters such as the injected energy, the ejecta mass, the torus mass, and the initial opening angles by conducting two-dimensional hydrodynamical simulations together with neutrino transport. We find that the typical value of the opening angles inferred from the analysis of the observed SGRBs can be reproduced in our parameter space. On the other hand, other mechanisms or parameter range may be needed to make the opening angle more than 20 degree.

5. Schedule and prospect for the future

As we mention in the previous section, some SGRBs are suggested to originate from the relativistic jet having a larger opening angle. We plan to extend our modeling to the three-dimensional simulation, which can avoid the numerical artifact arising from the assumption of axisymmetry, which can resolve the accumulation of heavy ejecta that remains on the top of the jet. This may broaden the jet opening angle.

We will also calculate the SGRB using the resultant jet profiles if our results can reproduce the observed signals.